ERDC/GSL TR-13-16

Geotechnical and Structures Laboratory

US Army Corps
of Engineers®
Engineer Research and
Development Center

ERDC
INNOVATIVE SOLUTIONS
for a safer, better world

Design and Synthesis of Bio-Inspired Nanocomposites

Synthesis of Carbonate-Based Micro/ Nanoscale Particles With Controlled Morphology and Mineralogy

Kevin Torres-Cancel, Robert D. Moser, Charles A. Weiss, Jr.,
Paul G. Allison, Mei Q. Chandler, Omar R. Rodriguez,
and Philip G. Malone

April 2013

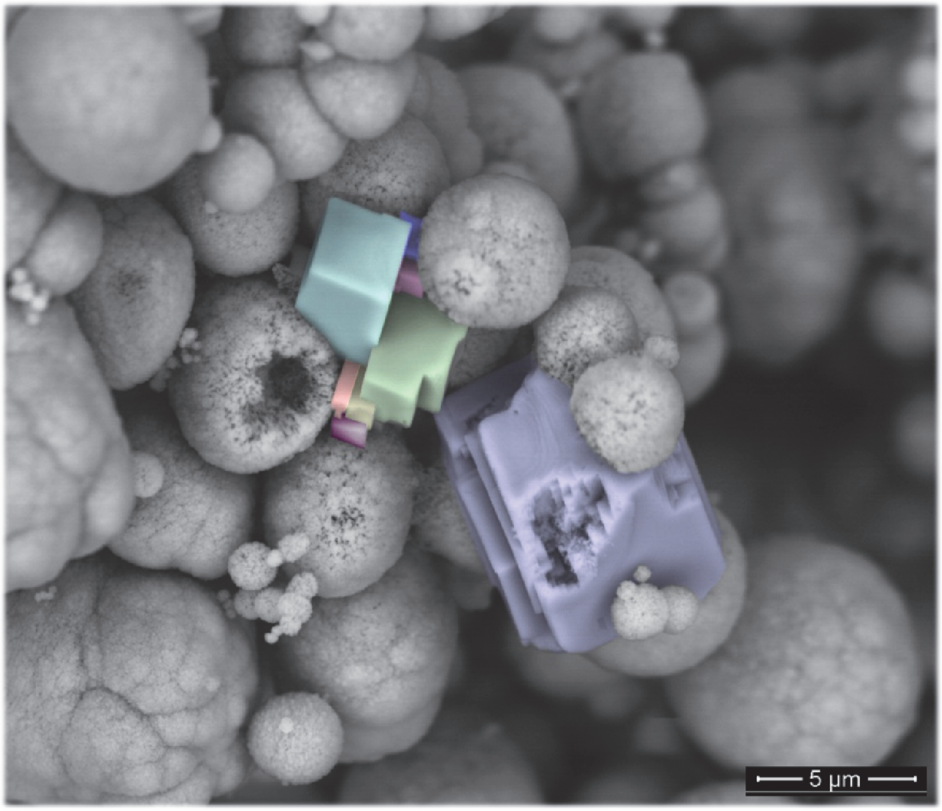

Design and Synthesis of Bio-Inspired
Nanocomposites

ERDC/GSL TR-13-16
April 2013

Synthesis of Carbonate-Based Micro/Nanoscale Particles With Controlled Morphology and Mineralogy

Kevin Torres-Cancel, Robert D. Moser, Charles A. Weiss, Jr.,
Paul G. Allison, Mei Q. Chandler, and Philip G. Malone

Geotechnical & Structures Laboratory
US Army Engineer Research and Development Center
3909 Halls Ferry Road
Vicksburg, MS 39180

Omar R. Rodriguez

Department of Mechanical Engineering
259 Boulevard Alfonso Valdes
University of Puerto Rico
Mayagüez, PR 00680

Final report

Prepared for Headquarters, US Army Corps of Engineers
Washington, DC 20314-1000

Under Work Unit 6430DL

Abstract

Biological structural materials such as bone, nacre and fish scales utilize unique material structures and chemistry, especially nanoscale structures to provide high strength as well as high ductility. To incorporate these design principles into the material design, novel synthesis methods need to be developed to fabricate composites with controlled morphology, orientation, organization and chemistry at nanoscale. In this study, the mineralogy and morphology of carbonate-based micro/nanoscale particles precipitated by reacting $(NH_4)2CO_3$ with mixed Ca, Sr, Mg, and Mn-acetates was investigated. As the proportion of the non-Ca component increased, the products shifted toward double carbonates and mixtures of double carbonates with single carbonates. Characterization by Scanning Electron Microscopy (SEM) and X-Ray Diffraction (XRD) to determine crystal sizes, morphology, and structure of precipitated phases indicated a potential for re-crystallizing the products to form new composite materials. Ongoing research efforts are focused on using information obtained in the present study to develop composites by hydrothermal recrystallization of metastable phases.

Contents

Figures and Tables

Figures

Table

Preface

This study was conducted for and funded by the Center Directed Research Program, under Project Number, 6430DL, “Design and Synthesis of Bio-Inspired Nanocomposites. The technical monitors were Dr. Jeffery P. Holland and Dr. John M. Cullinane .

The work was performed by the Concrete and Materials Branch (GM-C) of the Engineering Systems and Materials Division (GM) and Structural Mechanics Branch (GS-M) of the Geosciences and Structures Division (GS), US Army Engineer Research and Development Center – Geotechnical and Structures Laboratory (ERDC-GSL).

At the time of publication, Christopher Moore was Chief, Concrete and Materials Branch; Dr. Will McMahon was Chief, Structural Mechanics Branch; Dr. Larry N. Lynch was Chief, Engineering Systems and Materials Division; Bart P. Durst was Chief, Geosciences and Structures Division; and Dr. David Horner was the Technical Director for Military Engineering. The Deputy Director of ERDC-GSL was Dr. William P. Grogan and the Director was Dr. David W. Pittman.

COL Kevin J. Wilson was the Commander of ERDC. Dr. Jeffery P. Holland was the Director.

1 Introduction

Structural biomaterials such as nacre, bone, and fish scales all possess structures that have hierarchical spatial configurations (Espinosa et al. 2009; Bruet et al. 2008). The basic building blocks of the biomaterials are in the nanometer size range, because nanometer-size particles are flaw-insensitive due to geometry confinement (Gao et al. 2003). The basic building blocks of biomaterials are inorganic materials such as aragonite or phosphate, arranged as composites with polymer material created from proteins. The carbonate or phosphate components are intrinsically brittle by themselves but create amazingly tough composites when bonded in orderly layers by soft organic materials. The resulting nanocomposites have both strength and ductility several orders of magnitude higher than the individual constituents (Barthelat 2007). Current man-made composites usually involve layered schemes measuring on the order of millimeters. Cementitious composites have limited control in the morphology and order of constituents at all scales. This is the reason that materials such as ceramics and cementitious composites are lacking in ductility and tensile strength and are limited to applications where compressive stresses prevail. Achieving the kind of optimization of ductility and tensile strength similar to biomaterials requires the spatial ordering of laminates, but with the correct contrast in properties applied at the nanometer scale.

Biomaterials such as nacre, bone, and fish scale have revealed what effective arrangements of materials should be at the nanoscale. The nacre exhibits inorganic platelets oriented parallel to the surface in a brick-mortar style (Espinosa et al. 2009). The hard inorganic platelet in nacre has dimensions of approximately eight mm in length and width, and a couple of hundred nanometers in thickness (Espinosa et al. 2009). A thin layer of soft organic material bonds the platelets with thicknesses of approximately 40 nm (Espinosa et al. 2009). When nacre deforms under load, the inorganic platelets slide over each other like dislocations in ductile metals. The nanosized thickness of inorganic platelets ensures that the material deforms by inter-particle sliding, rather than fracturing of individual particles, thus providing plasticity similar to dislocations in ductile metals. Furthermore, the nanosized thickness of inorganic platelets allows a maximum number of platelets to participate in the sliding, creating high dislocation density characteristic of ductile metals. The bridges between inorganic platelets provide strengthening by acting like second-phase particles in ductile metals. The unique protein layers between platelets have folding and unfolding mechanisms to provide maximum energy dissipation.

The question arises: How can we take advantage of what we have learned from nature to produce materials with exceptional properties? Biomaterials are built in a bottom-up approach, atom-by-atom through a process directed by the organism's DNA. It is not clear how these structures can be reproduced through inorganic processes. Researchers have been attempting to produce nacre-like composites by using either bottom-up or top-down approaches. For example, Lin et al. (2010) have used electrophoretic deposition technology to assemble surface-roughened inorganic nanoplatelets into ordered multilayers that mimic the brick-and-mortar nanostructure found in nacre. Launey et al. (2009) have used a top–down approach to build nacre-like ceramics by using an ice-templated structure. Both research efforts produced materials with much higher ductility and tensile strength than their individual components. However, the thicknesses of the basic building blocks of the composites by Launey et al. (2009) are limited to the micron range and the bonding layer is also much thicker than the tens of nanometers found in nacre. Lin et al. (2010) achieved nanosize-thick particles, but were not able to make the bridges between the nanoparticles. Neither effort has achieved the level of load transfer as seen in nacre.

The primary mineral phase in nacre and calcium carbonate occurs primarily in three crystalline forms; calcite, aragonite, and vaterite. In the case of nacre, the aragonite polymorph is predominant. The most stable form of calcium carbonate in earth surface conditions is calcite. There is no abundant natural source of vaterite. Mixed alkaline-earth phases such as strontium or magnesium-rich carbonates also are not common. All of the low- stability carbonates are useful, since their morphology and crystal structure can produce mineral bonding, making them important components for use in specialized cements and coatings. Nanoparticulate vaterite, for example, is applied to specialized paper products to make highly absorbent surfaces. Low-stability carbonates are most useful when they form fine crystals of a particular morphology (for example, needle-like aragonite) or composite structures such as calcite spherules composed of nanocrystals. Yamasaki et al. (1993) showed that metastable carbonate in the form of fine crystal aggregates can be recrystallized to form novel composites.

This report discusses rapid carbonate precipitation systems that can produce metastable carbonates with the structure, morphology, and decomposition characteristics that allow them to be used as nanoscale building blocks to construct hierarchical composite materials. Based on this study, ongoing research is focusing on utilizing indentified metastable carbonates to develop composite materials using various hydrothermal recrystallization techniques to promote the transformation of metastable phases to oriented stable phases while also incorporating a polymeric matrix.

2 Materials and Methods

The procedure for producing metastable, nanocrystalline carbonates was adapted from the precipitation protocol outlined in Prah et al. (2011). In addition to calcium acetate alone, mixtures of calcium acetate, strontium acetate, magnesium acetate, or manganese acetate were also used in the procedure. The general reaction proceeds as follows:

$$\left(\mathrm{NH_4}\right)_2\mathrm{CO_3} + \left(\mathrm{M,Ca}\right)\left(\mathrm{C_2H_3O_2}\right)_2 \rightarrow \left(\mathrm{M,Ca}\right)\mathrm{CO_3} + 2\,\mathrm{NH_4C_2H_3O_2} \tag{1}$$

where “M” is Sr, Mg, or Mn. Pure calcium carbonate samples were prepared by mixing equimolar solutions of reagent grade calcium acetate and ammonium carbonate (ACS grade) in deionized H_2O at a controlled rate. A 0.5-M calcium acetate solution was added to a stirred ammonium carbonate solution of equal volume and equal molarity using a variable-flow peristaltic pump set up to deliver 25 ml/min. The reaction was conducted at a constant temperature of 25° C. All of the precipitates prepared with calcium acetate mixed with strontium, magnesium, or manganese acetates were prepared in a similar procedure. A 0.5-M calcium acetate solution containing a 0.1-M, 0.2–M, or 0.5-M concentration of the interfering ion (i.e., Sr, Mg, or Mn) was added to a 0.5-M ammonium carbonate solution at a rate of 25 ml/min with constant stirring at 25° C. Each of the resulting suspensions was filtered through filter paper (2.5 mm pores, Whatman no. 42). The precipitate was rinsed with deionized water and dried for four hours at 105° C. The precipitates were all below 44 mm (sieve size, 325-mesh) and could be mounted in sample holders for X-ray diffraction (XRD) measurements without grinding. XRD patterns were obtained using a Panalytical X’Pert Pro diffractometer using iron-filtered cobalt radiation, and analyzed using Panalytical X’Pert HighScore Plus and MDI Jade software packages. Imaging with scanning electron microscopy (SEM) of the resulting double carbonates was performed using an FEI Nova NanoSEM 630 field-emission variable-pressure SEM at an accelerating voltage of 5-kV and chamber pressure of 0.1 mbar.

3 Results

The chemical composition, grain sizes, and morphology of the crystals precipitated from the different reactions were analyzed. Rapidly mixing reactants at high concentrations, at room temperatures (25° C), and at elevated pH levels typically precipitate metastable crystalline phases, such as vaterite, as small-sized particles or spheroidal arrays of nanocrystals. Prah et al. (2011) reported the precipitation of spheroidal vaterite using concentrated ammonium carbonate and calcium-containing reactants. Recrystallization and changes in shapes of agglomerated grains can occur if the solids are not separated from the suspension. Table 1 shows a summary of the mineral composition, size, and shape of the precipitates produced from different reactions. The solid phases reported in Table 1 include the original precipitated phases and the phases that form following filtration, rinsing, and drying.

Table 1. Results of precipitation reaction.

Starting Materials	Mineral Composition	Grain Shape	Grain size (μm)
Ca only	calcite	Clusters of rhombohedra	10-20
0.1-M Sr	calcite, aragonite, vaterite, strontianite	Small rhombohedra, lath-like crystals	< 1
0.2-M Sr	calcite, calcium-rich strontianite	Rhombohedra, lath-like crystals	<1
0.5-M Sr	strontianite strontium-rich calcite	Agglomerations of spheroids	20-30
0.1-M Mg	Calcite	Agglomerations of spheroids, sheets of amorphous carbonate gel	1 to 2
0.2-M Mg	calcite	Agglomerations of spheroids	<1
0.5-M Mg	Magnesium-rich calcite	Agglomerations of spheroids	<1
0.1-M Mn	calcite, manganese-rich calcite	Spherical agglomerations of rhombohedra	10 to 15
0.2-M Mn	calcite, mangano-calcite	Spherical agglomerations of rhombohedra	10 to 15
0.5-M Mn	kutnohorite	Smooth spheroids, micro-crystals	5 (spheroids) <1 (nanocrystals)

The product found in the filtered and dried Ca-only precipitate was a single polymorph, calcite, as shown in Figure 1(a), in the form of fine (10-20 µm diam.) spherical clusters, as shown in Figure 2. The shape of the clusters of rhombohedra is similar to the shape of the clusters formed from the recrystallization of the classic metastable vaterite spheroids produced by other investigators (Prah et al. 2011).

As the ratio of calcium to strontium, magnesium, or manganese increased in each experimental series, the cation competing with calcium becomes more prominent in the final products.

Figure 1(b) shows that aragonite appeared at the low concentrations of Sr; but as the ratio of Sr ions to Ca ions increases, strontium-rich calcite and strontianite (Figure 1(d)) make up a large portion of the precipitates. The precipitates were a mixture of rhombohedra and lath-like crystals when Sr concentration was 0.1-M, as shown in Figure 3(a). The size of the crystals was in the order of hundreds of nanometers. When the Sr concentration increased to 0.2-M, most of the precipitates were calcium strontianite, as shown in Figure 1(c). The shape of the crystals was mainly lath-like, and the size of the crystals was in the order of the hundreds of nanometers, as shown in Figure 3(b). When the Sr concentration increased to 0.5-M, the precipitates were mainly strontianite, as shown in Figure 1(d). The morphology of the precipitates became spheroid with the size of the particles in the order of 10-20 microns, as shown in Figure 3(c). The results from synthetic samples are consistent with the usual composition of the corresponding minerals. The utilization of the strontium ion in Ca-rich solution to produce aragonite was noted by Sunagawa et al. (2007). The strontium content in natural aragonite does not exceed l-2 mol percent whereas strontianite can contain up to 25-30 mol percent substituted calcium ion (Speer 1983). Increasing the proportion of Sr favors the formation of strontianite.

Figure 1(e-g) and Figure 4(a-c) show the progression in composition and shape of precipitates from spheroids of calcite and amorphous calcium carbonate at the lowest Mg addition to spheroids of magnesium calcite with an increasing proportion of Mg. When the Mg concentration was 0.1-M, the precipitates mainly included calcites and amorphous calcium carbonates, as shown in Figure 1(e). Figure 4(a) shows that the morphologies of the calcite agglomerates are spheroids with size in the order of hundreds of nanometers. The amorphous calcium carbonate had a sheet-like morphology. When the Mg concentration was 0.2-M, the precipitates mainly include

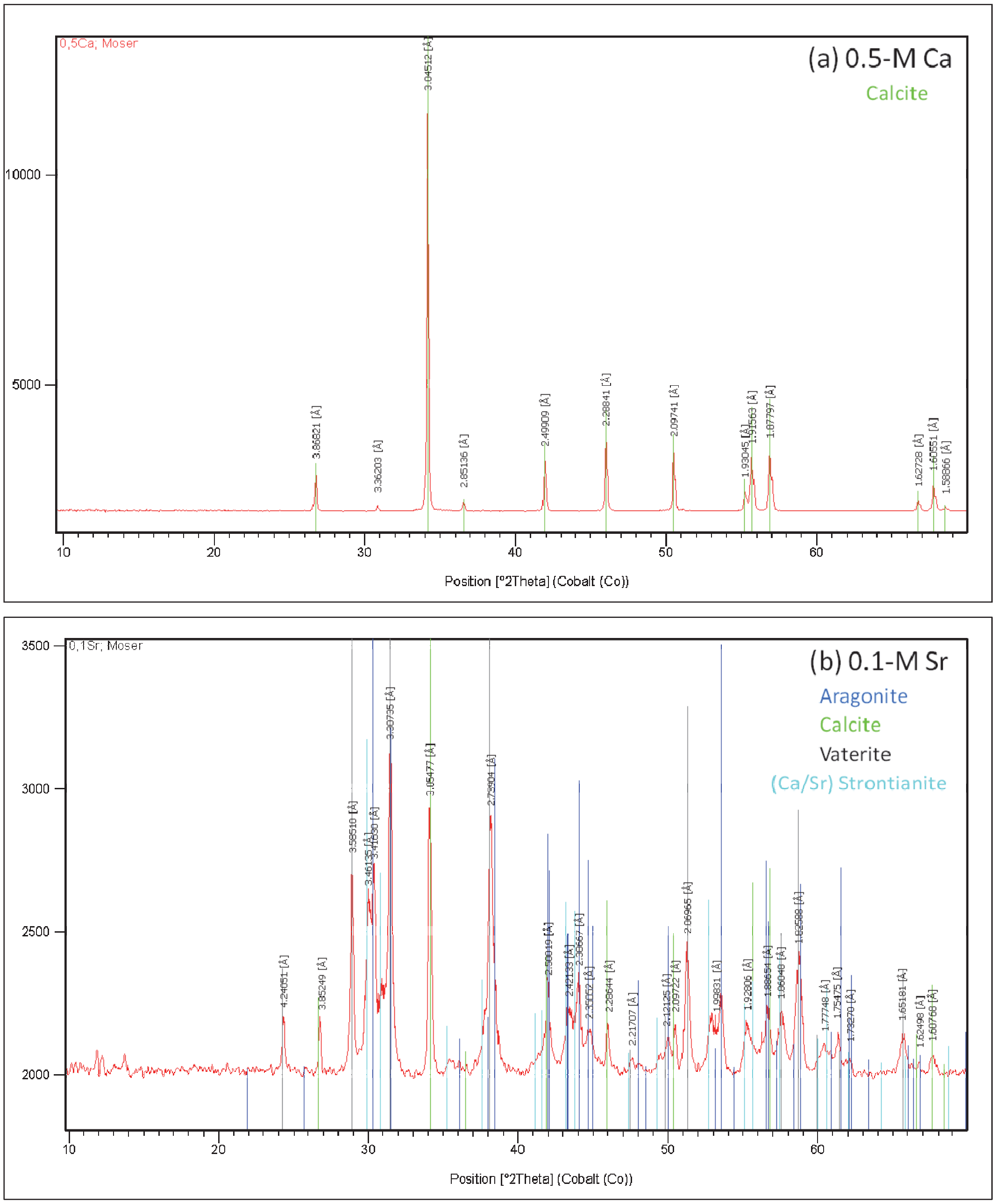

Figure 1. XRD patterns for Ca-only, and Ca/Sr, Ca/Mg, and Ca/Mn carbonates (continued).

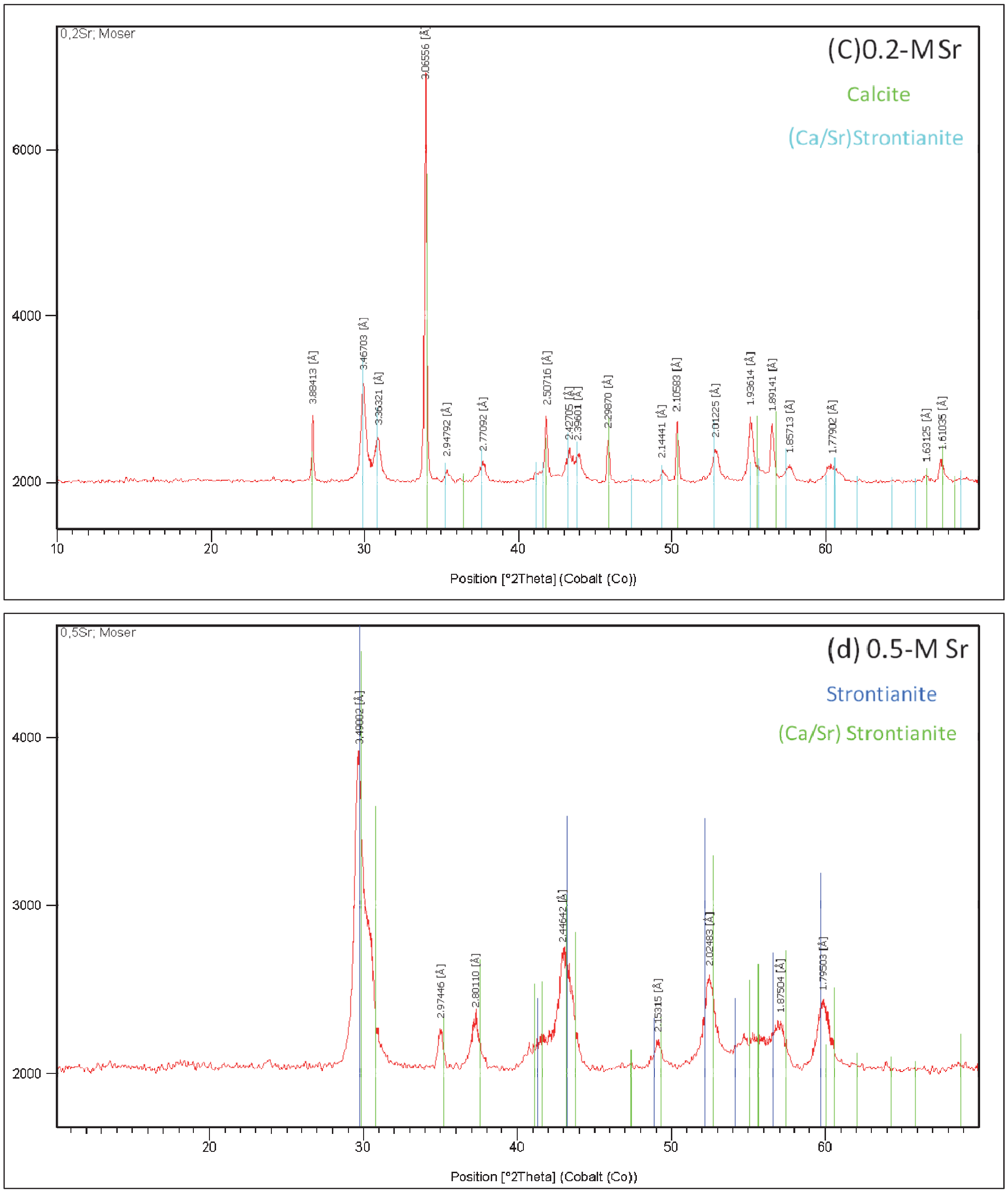

Figure 1. (continued).

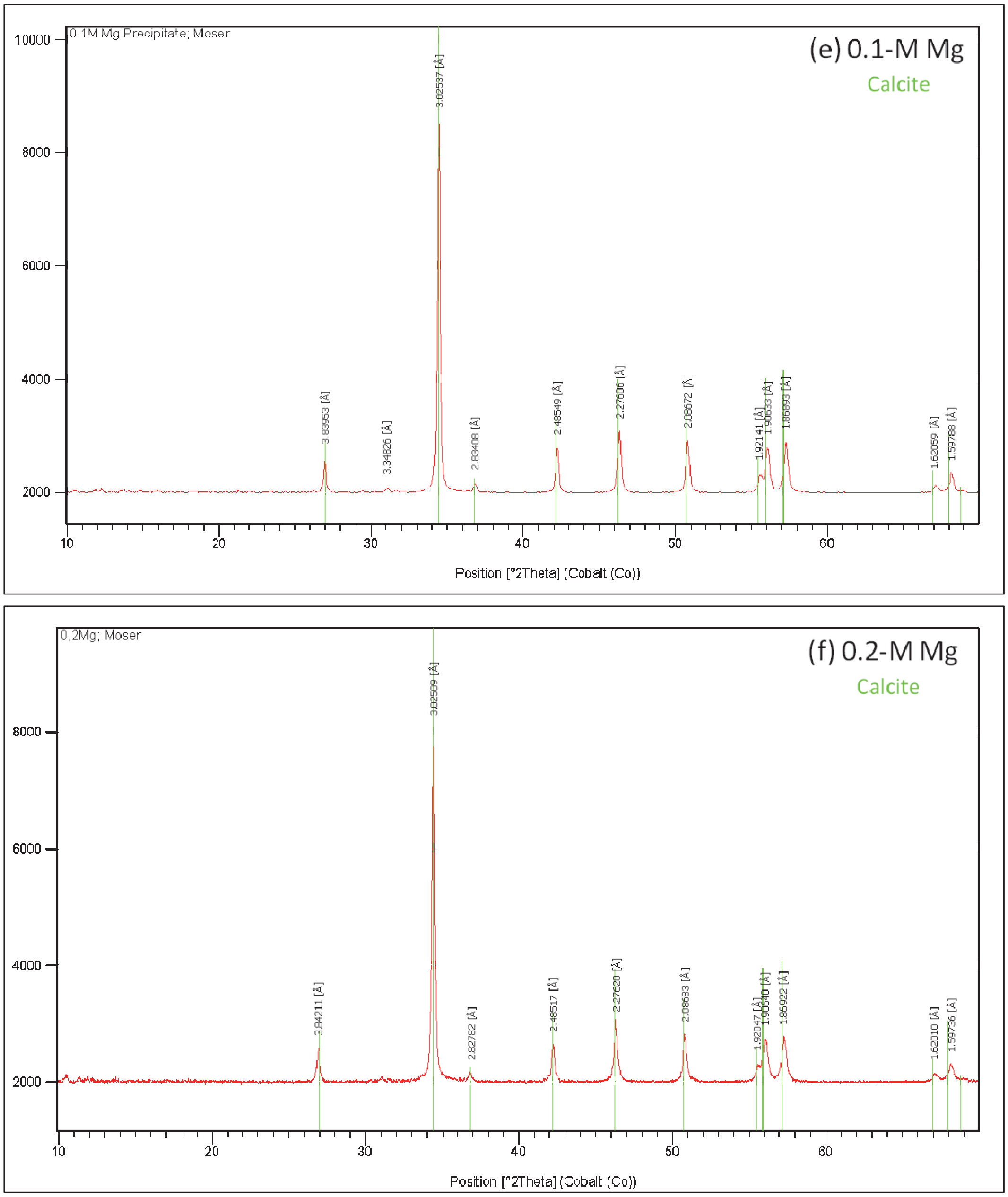

Figure 1. (continued).

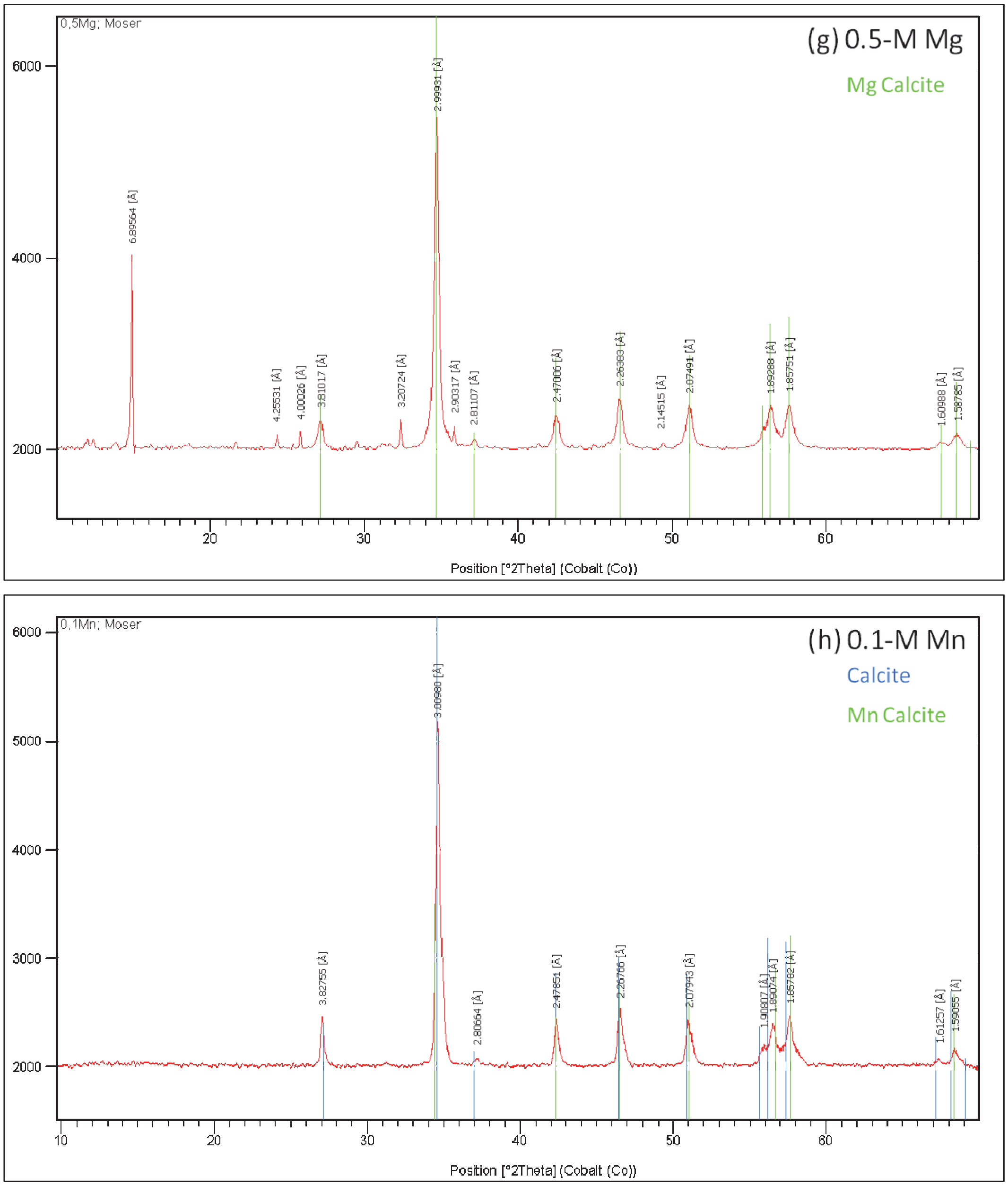

Figure 1. (continued).

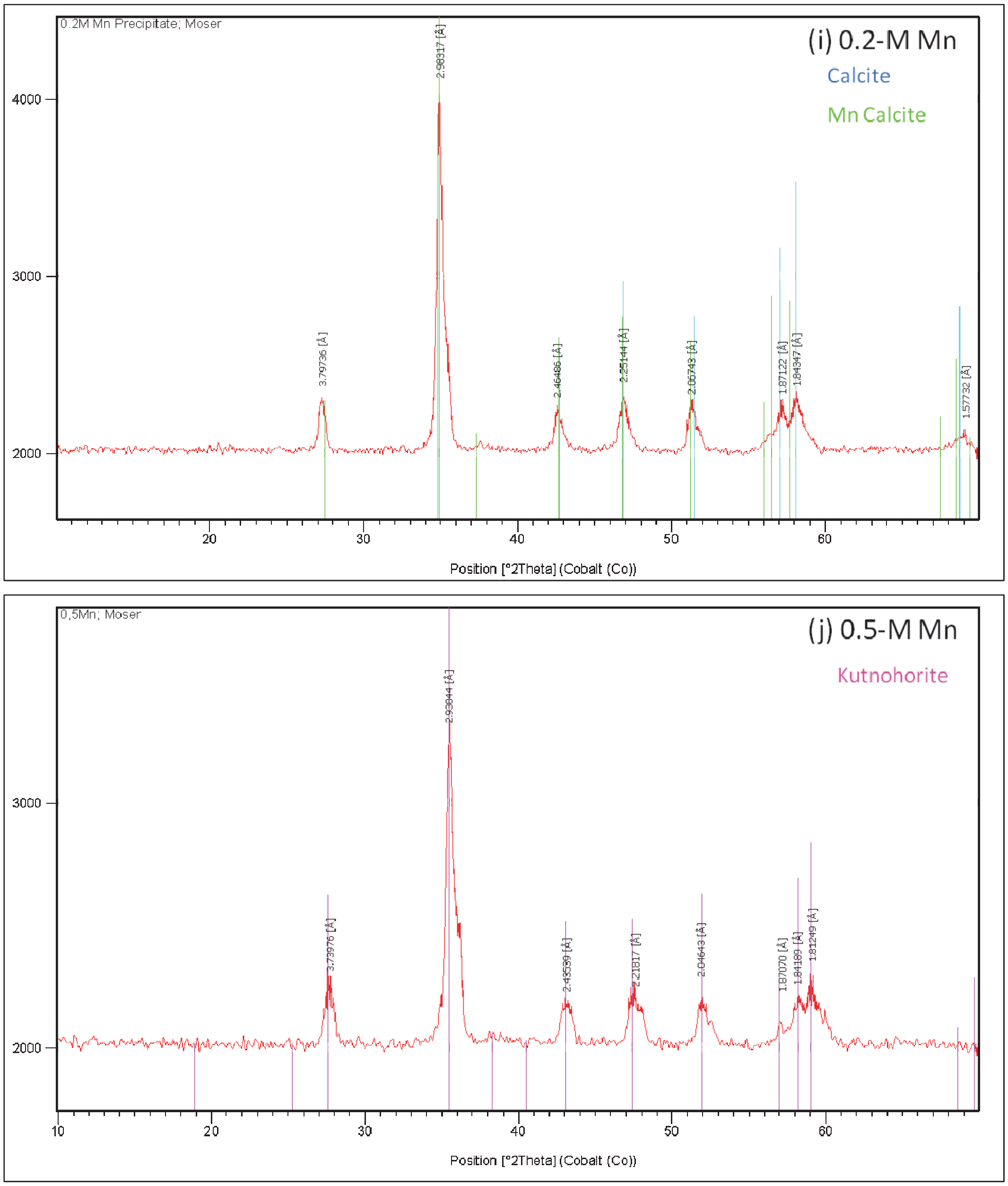

Figure 1. (concluded).

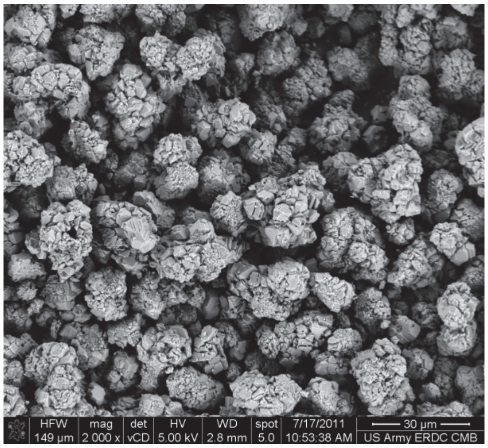

Figure 2. Precipitates from the calcium acetate-ammonium carbonate reaction.

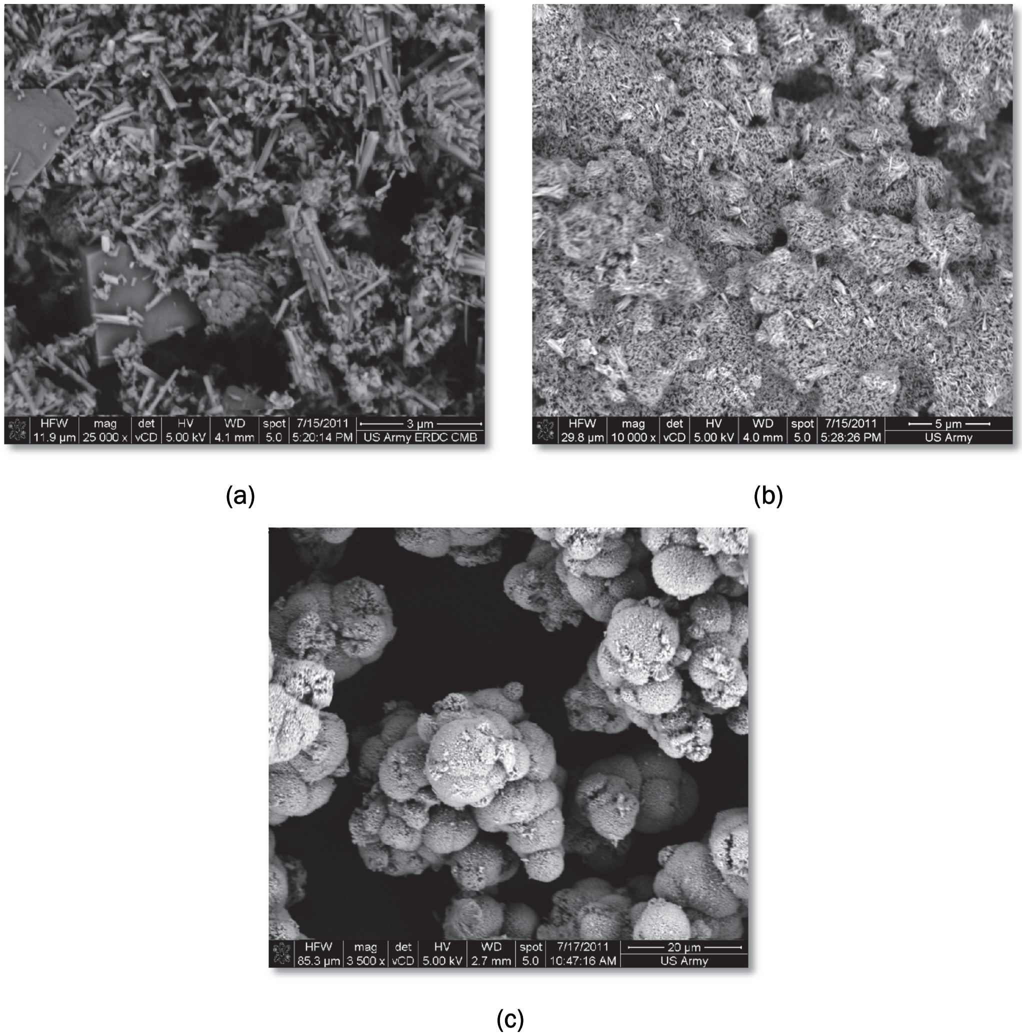

Figure 3. Precipitates produced with an increasing concentration of Sr include (a) mixed rhombohedra and lath-like crystals with 0.1-M Sr, (b) fine lath-like crystals with 0.2-M Sr, and (c) agglomerations of spheroids with 0.5-M Sr.

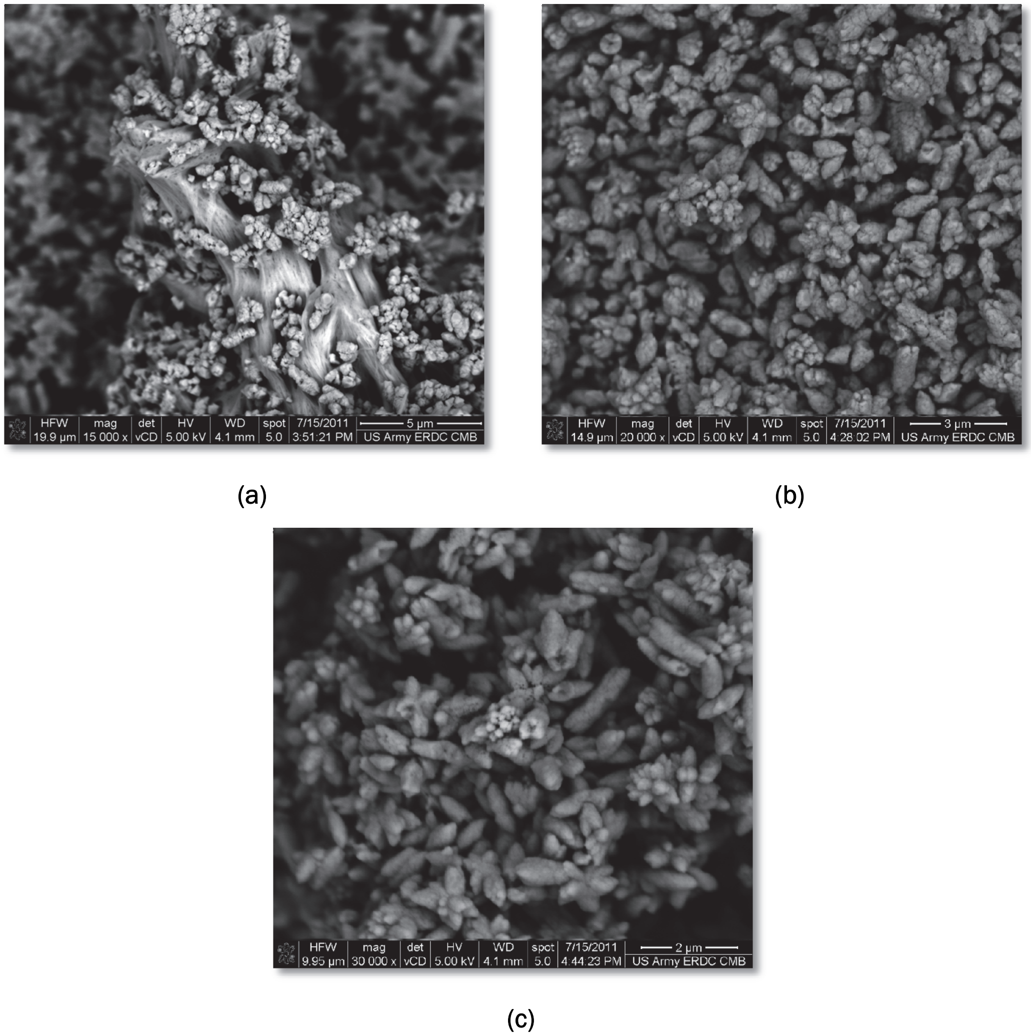

(a) (b)

(c)

Figure 4. Precipitates produced with an increasing concentration of Mg include (a) small spheroids of calcite and amorphous calcium carbonate with 0.1-M Mg, (b) spheroids of calcite with 0.2-M Mg, and (c) spheroids of magnesium-rich calcite with 0.5-M Mg .

calcite, as shown in Figure 1(d). The morphologies of the calcite agglomerates were spheroid with the size of the particles in the order of hundreds of nanometers, as shown in Figure 4(b). When the Mg concentration was 0.5-M, the precipitates included magnesium-rich calcite, as shown in Figure 1(e). The morphologies of the particles were also spheroid with the size in the order of hundreds of nanometers.

Figure 1(h-j) and Figure 5(a-c) show progression in composition and shape from large (10-15 µm) spheroids of calcite and manganese-rich calcite at the lowest Mn concentration to smooth nanosized spheroids of kutnohorite (double carbonate of Ca and Mn) as the proportion of Mn increased. When the Mn concentration was 0.1-M, the precipitates included calcite and manganese-rich calcite, as shown in XRD pattern Figure 1(h). The morphologies of the particles were spherical with the size of the diameters in the order of 20-30 microns, as shown in Figure 5(a). When the Mn concentration was 0.2-M, the precipitates included calcite and manganocalcite, as shown in XRD pattern Figure 1(i). The morphologies of the particles included spherical-shaped agglomeration of calcite rhombohedra with diameters in the order of 10-15 microns and some fine crystals with the crystal size in the order of less than one micron, as shown in Figure 5(b). When the Mn concentration was 0.5-M, the precipitates included only kutnohorite. The morphologies of the precipitates were spherical with averaged diameters of a few microns or less than one micron (nanosized), as shown in Figure 5(c).

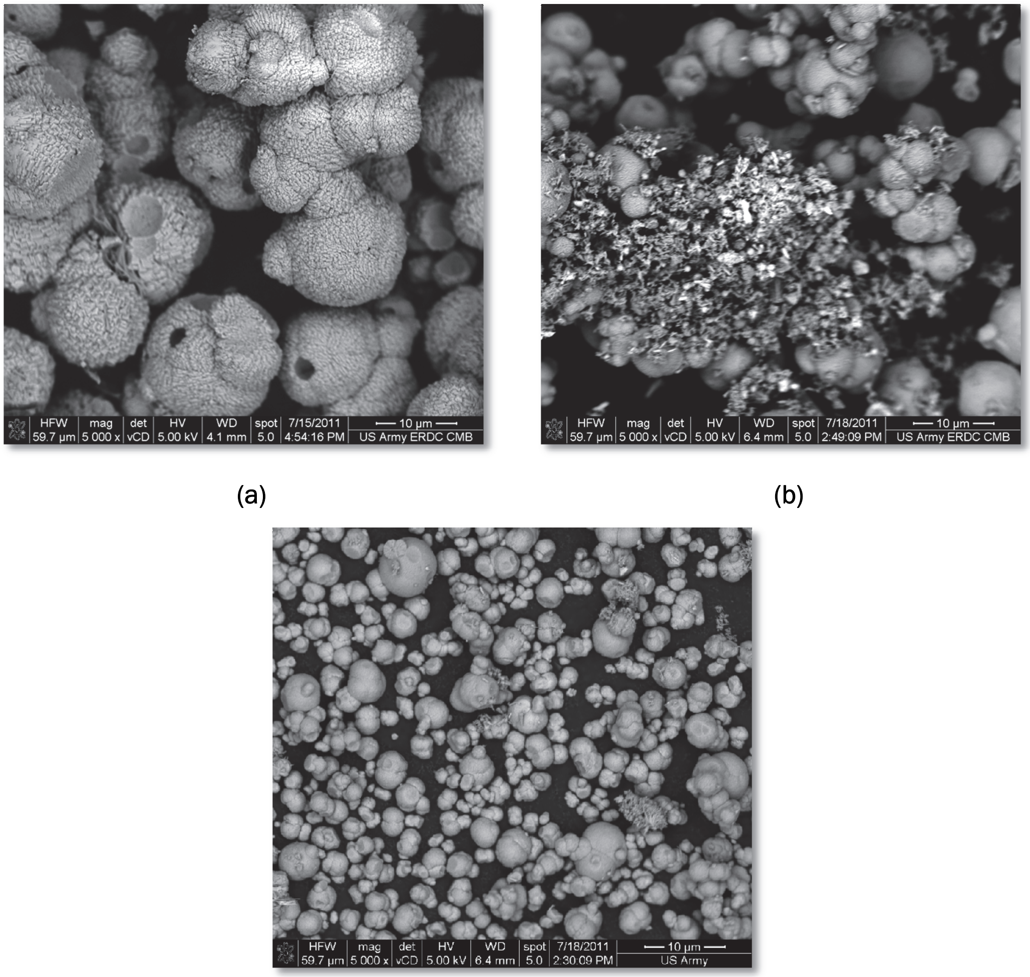

(a) (b)

(c)

Figure 5. Precipitates produced with an increasing concentration of Mn include (a) spherical agglomerations of rhombohedra with 0.1-M Mn, (b) spherical agglomerations and fine crystals with 0.2-MMn, and (c) smooth spherical agglomerations of kutnohorite with 0.5-M Mn.

4 Conclusions

A variety of useful metastable and mixed composition carbonate phases can be produced by reacting ammonium carbonate and mixed calcium acetate that was combined with strontium, magnesium, or manganese acetates. The major features that were observed in these carbonate production trials were:

1. Operations that produce the small crystallites suitable for use in cementing or recrystallization could be conducted at reasonable temperatures (25^o C) using modest stirring and mixing rates.
2. With the exception of unblended calcium acetate, fine-grained or spherical aggregates of very fine crystals could be obtained.
3. As expected, the more concentrated the non-calcium component is, the more that it was partitioned into the carbonate phases.
4. Manganese acetate was the only reactant that could produce a double carbonate with calcium in the form of pure kutnohorite.

References

Barthelat, F. 2007. Biomimetics for next generation materials. Philosophical Transactions of the Royal Society A 2007; 365: 2907-2919.

Bruet, B. J. F., J. Song, M. C. Boyce, and C. Ortiz. 2008. Material design principles of ancient fish armour. *Nature materials(7)748-56.*

Espinosa, H. D., J. E. Rim, F. Barthelat, J. Markus, and M. J. Buehler. 2009. Merger of structure and material in nacre and bone - Perspectives on de novo biomimetic materials. *Progress in Materials Science* (54)1059-1100.

Gao, H., B. Ji, I. L. Jäger, E. Arzt, and P. Fratzl. 2003. Materials become insensitive to flaws at nanoscale: Lessons from nature. In *Proceedings of the National Academy of Science* (100)5597-5600.

Launey, M. E., E. Munch, D. H. Alsem, H. B. Barth, and E. Saiz. 2009. Designing highly toughened hybrid composites through nature-inspired hierarchical complexity. *Acta Materialia* (57)2919-32.

Lin, T. H., W. H. Huang, I. J. Jun, P. Jiang. 2010. Bioinspired assembly of surface-roughened nanoplatelets. *Journal of Colloid and Interface Science* (344)272-78.

Prah, .J, J. Maček, and G. Dražič. 2011. Precipitation of calcium carbonate from a calcium acetate and ammonium carbamate batch system. *Journal of Crystal Growth* (324)229-34.

Speer, J. 1983. Crystal chemistry and phase relations of orthorhombic carbonates. *Reviews in Mineralogy:Carbonates: Mineralogy and Chemistry* (11)145-90.

Sunagawa, I., Y. Takahashi, and H. Imai. 2007. Strontium and aragonite-calcite precipitation. *Journal of Mineralogical and Petrological Science* (102)174-81.

Yamasaki, N., T. Weiping, and K. Yanagisawa. 1993. Solidification of CaCO3 containing SrCO3 by hydrothermal hot-pressing. *Journal of Materials Research* (8)1972-76.

Appendix A: Thermogravimetric Analysis

In addition to XRD and SEM, investigations of synthesized carbonate, thermogravimetric analysis (TGA) was also conducted on each material to investigate phases formed and their respective stability. Thermal analysis measurements were performed on a Netzsch TG 449 F1 Jupiter combined TGA/DSC from 25-1000° C at a temperature ramp rate of 10° C/min. The following presents results of TGA studies of each material.

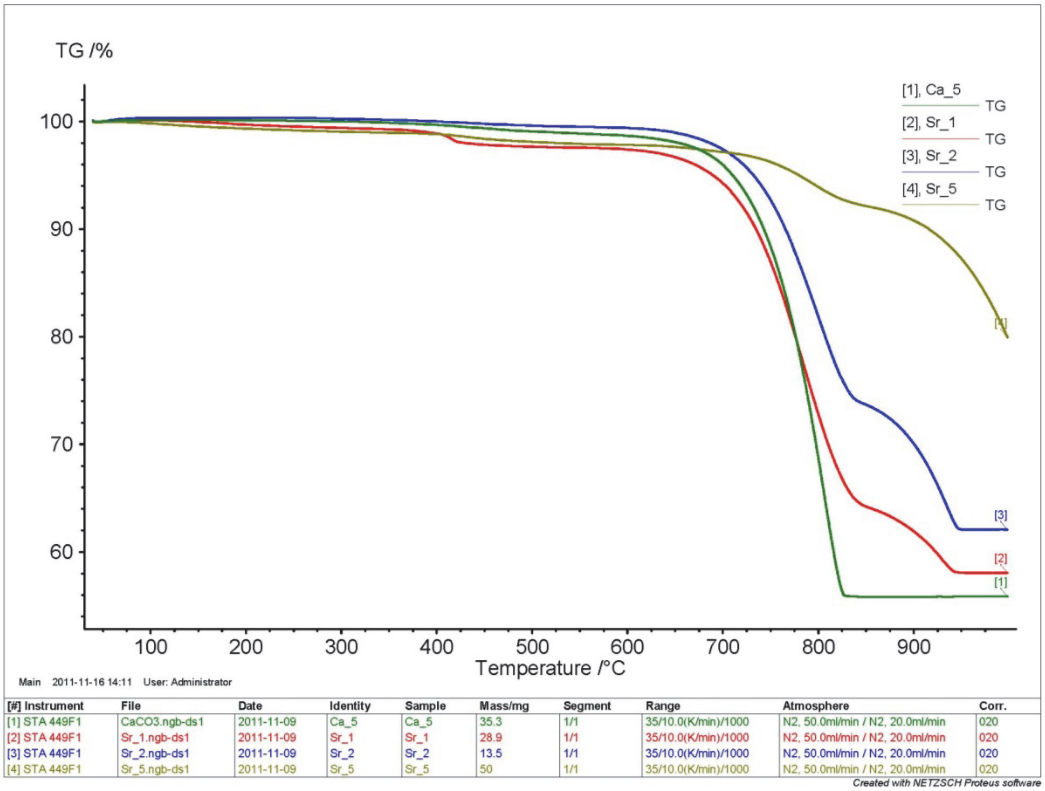

[#] Instrument	File	Date	Identity	Sample	Mass/mg	Segment	Range	Atmosphere	Corr.
[1] STA 449F1	CaCO3.ngb-ds1	2011-11-09	Ca_5	Ca_5	35.3	1/1	35/10.0(K/min)/1000	N2, 50.0ml/min / N2, 20.0ml/min	020
[2] STA 449F1	Sr_1.ngb-ds1	2011-11-09	Sr_1	Sr_1	28.9	1/1	35/10.0(K/min)/1000	N2, 50.0ml/min / N2, 20.0ml/min	020
[3] STA 449F1	Sr_2.ngb-ds1	2011-11-09	Sr_2	Sr_2	13.5	1/1	35/10.0(K/min)/1000	N2, 50.0ml/min / N2, 20.0ml/min	020
[4] STA 449F1	Sr_5.ngb-ds1	2011-11-09	Sr_5	Sr_5	50	1/1	35/10.0(K/min)/1000	N2, 50.0ml/min / N2, 20.0ml/min	020

Figure A-1. TGA results for $CaCO_3$ (baseline), and carbonates with addition of 0.1-, 0.2-, and 0.5-M Sr along with Ca. In Ca-only case, mass loss at ~800 °C associated with loss of CO_2 from $CaCO_3$ ($CaCO_3 \rightarrow CaO + CO_2$). With addition of Sr, multi-phase behavior is observed due to mixture of calcium carbonate polymorphs (i.e., calcite, vaterite) along with Sr-containing phases.

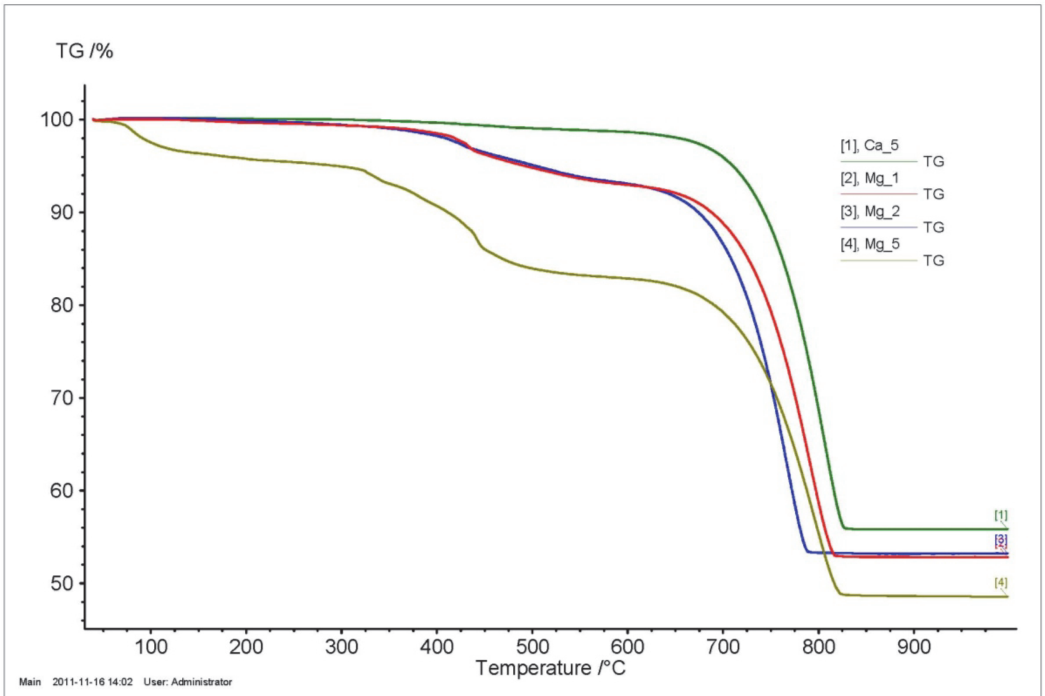

[#] Instrument	File	Date	Identity	Sample	Mass/mg	Segment	Range	Atmosphere	Corr.
[1] STA 449F1	Ca_5.ngb-ds1	2011-11-09	Ca_5	Ca_5	35.3	1/1	35/10.0(K/min)/1000	N2, 50.0ml/min / N2, 20.0ml/min	020
[2] STA 449F1	Mg_1.ngb-ds1	2011-11-10	Mg_1	Mg_1	37.4	1/1	35/10.0(K/min)/1000	N2, 50.0ml/min / N2, 20.0ml/min	020
[3] STA 449F1	Mg_2.ngb-ds1	2011-11-10	Mg_2	Mg_2	19	1/1	35/10.0(K/min)/1000	N2, 50.0ml/min / N2, 20.0ml/min	020
[4] STA 449F1	Mg_5.ngb-ds1	2011-11-10	Mg_5	Mg_5	48.6	1/1	35/10.0(K/min)/1000	N2, 50.0ml/min / N2, 20.0ml/min	020

Created with NETZSCH Proteus software

Figure A-2. TGA results for $CaCO_3$ (baseline), and carbonates with addition of 0.1-, 0.2-, and 0.5-M Mg along with Ca. In Ca-only case, mass loss at ~800 °C associated with loss of CO_2 from $CaCO_3$ ($CaCO_3 \rightarrow CaO + CO_2$). With addition of 0.1- and 0.2- M Mg, the onset of multi-phase behavior is observed with the primary mass loss occurring due to loss of CO2 with a reduction in loss temperature with increasing Mg composition (supported by XRD results). At 0.5- M Mg, multi-phase behavior is observed with mixing between Mg-calcite and Ca-only calcite.

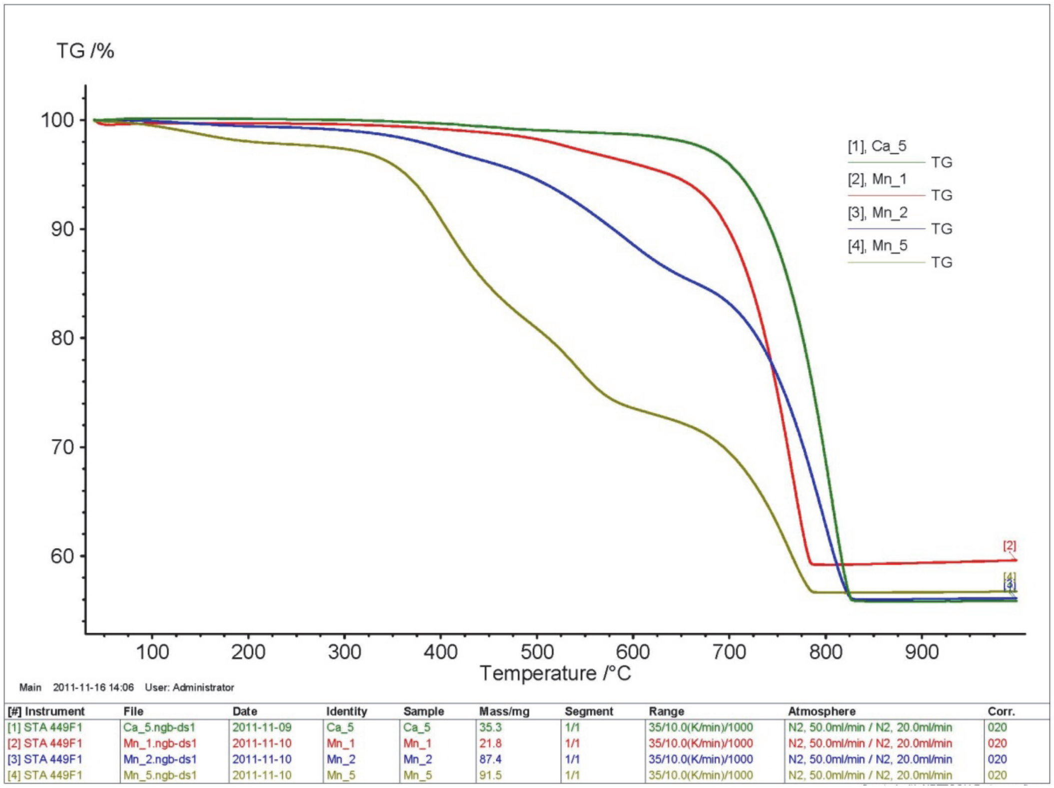

[#] Instrument	File	Date	Identity	Sample	Mass/mg	Segment	Range	Atmosphere	Corr.
[1] STA 449F1	Ca_5.ngb-ds1	2011-11-09	Ca_5	Ca_5	35.3	1/1	35/10.0(K/min)/1000	N2, 50.0ml/min / N2, 20.0ml/min	020
[2] STA 449F1	Mn_1.ngb-ds1	2011-11-10	Mn_1	Mn_1	21.8	1/1	35/10.0(K/min)/1000	N2, 50.0ml/min / N2, 20.0ml/min	020
[3] STA 449F1	Mn_2.ngb-ds1	2011-11-10	Mn_2	Mn_2	87.4	1/1	35/10.0(K/min)/1000	N2, 50.0ml/min / N2, 20.0ml/min	020
[4] STA 449F1	Mn_5.ngb-ds1	2011-11-10	Mn_5	Mn_5	91.5	1/1	35/10.0(K/min)/1000	N2, 50.0ml/min / N2, 20.0ml/min	020

Figure A-3. TGA results for $CaCO_3$ (baseline), and carbonates with addition of 0.1-, 0.2-, and 0.5- M Mn along with Ca. In Ca-only case, mass loss at ~800 °C associated with loss of CO_2 from $CaCO_3$ ($CaCO_3 \rightarrow CaO + CO_2$). At 0.1- M Mn, behavior evident of material primarily composed of the polymorph calcite with a small reduction in CO_2 loss temperature. At 0.2- M Mn, a multiphase response is observed. When 0.5- M Mn was added, an almost complete loss in calcite was observed with corresponding XRD analyses that show the material is primarily composed of kutnohorite, a balanced Ca,Mn carbonate.

REPORT DOCUMENTATION PAGE

Form Approved
OMB No. 0704-0188

1. REPORT DATE *(DD-MM-YYYY)*
April 2013

2. REPORT TYPE
Final report

3. DATES COVERED *(From - To)*

4. TITLE AND SUBTITLE
Synthesis of Carbonate-Based Micro/Nanoscale Particles With Controlled Morphology and Mineralogy

5a. CONTRACT NUMBER

5b. GRANT NUMBER

5c. PROGRAM ELEMENT NUMBER

6. AUTHOR(S)
Kevin Torres-Cancel, Robert D. Moser, Charles A. Weiss, Jr., Paul G. Allison, Mei Q. Chandler, Omar R. Rodriguez, and Philip G. Malone

5d. PROJECT NUMBER

5e. TASK NUMBER

5f. WORK UNIT NUMBER
6430DL

7. PERFORMING ORGANIZATION NAME(S) AND ADDRESS(ES)

Geotechnical & Structures Laboratory
US Army Engineer Research and Development Center
3909 Halls Ferry Road
Vicksburg, MS 39180

Department of Mechanical Engineering
259 Boulevard Alfonso Valdes
University of Puerto Rico
Mayagüez, PR

8. PERFORMING ORGANIZATION REPORT NUMBER
ERDC/GSL TR-13-16

9. SPONSORING / MONITORING AGENCY NAME(S) AND ADDRESS(ES)
Headquarters, US Army Corps of Engineers
Washington, DC 20314-1000

10. SPONSOR/MONITOR'S ACRONYM(S)

11. SPONSOR/MONITOR'S REPORT NUMBER(S)

12. DISTRIBUTION / AVAILABILITY STATEMENT
Approved for public release; distribution is unlimited.

13. SUPPLEMENTARY NOTES

14. ABSTRACT

Biological structural materials such as bone, nacre and fish scales utilize unique material structures and chemistry, especially nanoscale structures to provide high strength as well as high ductility. To incorporate these design principles into the material design, novel synthesis methods need to be developed to fabricate composites with controlled morphology, orientation, organization and chemistry at nanoscale. In this study, the mineralogy and morphology of carbonate-based micro/nanoscale particles precipitated by reacting $(NH_4)2CO_3$ with mixed Ca, Sr, Mg, and Mn-acetates was investigated. As the proportion of the non-Ca component increased, the products shifted toward double carbonates and mixtures of double carbonates with single carbonates. Characterization by Scanning Electron Microscopy (SEM) and X-Ray Diffraction (XRD) to determine crystal sizes, morphology, and structure of precipitated phases indicated a potential for re-crystallizing the products to form new composite materials. Ongoing research efforts are focused on using information obtained in the present study to develop composites by hydrothermal recrystallization of metastable phases.

15. SUBJECT TERMS

Aragonite
Calcite
Calcium carbonate
Dopant
Mineralogy
Morphology
Precipitation
Vaterite

16. SECURITY CLASSIFICATION OF:			**17. LIMITATION OF ABSTRACT**	**18. NUMBER OF PAGES**	**19a. NAME OF RESPONSIBLE PERSON: Robert D. Moser**
a. REPORT	**b. ABSTRACT**	**c. THIS PAGE**			**19b. TELEPHONE NUMBER *(include area code)***
Unclassified	Unclassified	Unclassified	Unclassified	26	601-634-3261

Standard Form 298 (Rev. 8-98)
Prescribed by ANSI Std. 239.18